Global Simulation Accuracy Control in the Split-Step Fourier Simulation of Vector Optical Fiber Communication Channel

Qun Zhang[1], Santosh Karri[1], Muhammad Khaliq[1], Liudong Xing[2], and M. I. Hayee[3]
[1] Department of Electrical and Computer Engineering, Minnesota State University, Mankato, MN 56001, USA
[2] Department of Electrical and Computer Engineering, University of Massachusetts Dartmouth, MA 02747, USA
[3] Department of Electrical Engineering, University of Minnesota Duluth, Duluth, MN 55812, USA
Email: qun.zhang@mnsu.edu; lxing@umassd.edu; ihayee@d.umd.edu

Abstract—A symmetrized split-step Fourier (SSSF) simulation model with global simulation accuracy control is extended to vector optical fiber multi-span propagation cases, which are applicable to the waveform level simulation of polarization multiplexed coherent optical communication systems. Using local error bound obtained from a scalar simulation package, the prescribed global simulation accuracy can be satisfied for the simulation of propagation of optical signals with dual polarization input. Furthermore, it was found that the computational efficiency for one span simulation can be maintained for multi-span simulation. The developed simulation package can significantly speed up the time-consuming simulations which are typical in coherent optical fiber communication system design.

Index Terms—Optical fiber communications; coupled nonlinear Schrödinger (CNLS) equations; split-step fourier (SSF) method; computer simulation software package; polarization multiplexed QPSK (PM-QPSK)

I. Introduction

In the area of optical fiber communication systems design, it is crucial to enhance the computational efficiency of waveform level simulation [1] of optical signal propagation through the dispersive and nonlinear single mode fiber [2]. This is due to the fact that the optical communication system design is a multi-dimensional optimization problem. For traditional dispersion managed, intensity modulated direct detection (IMDD) based systems, signal launch power and dispersion map strength need to be optimized such that the system performance margin can be acceptable [3]. For each combination of optimizing parameter values such as launch power and dispersion compensation strength, waveform level simulation must be performed to probe system performance [4]. Fortunately, only thousands of pulses are simulated, and the detected photo voltage is assumed to have Gaussian statistics for the IMDD systems [5], [6]. For DPSK with interferometric based receiver (differentially coherent) systems, a modified Gaussian approximation can still be used for measuring reasonably large performance margin [7]. In contrast, the newly emerged coherent optical fiber communication systems usually require simulation of long runs of symbols up to the order of one million to estimate system performance via direct bit error counting. This is due to the presence of nonlinear devices such as signal clipping and quantization, and various adaptive signal processing used in the coherent receiver [8], [9]. Furthermore, optical fiber is a nonlinear channel and optical signals experience complex nonlinearity interaction with both the chromatic dispersion (CD) and polarization mode dispersion (PMD) [10], [11]. The need for simulating long waveforms represents a large computational burden in system design.

To handle the interplay between fiber Kerr nonlinearity and CD, split-step Fourier (SSF) based methods are often used [2]. By dividing a long optical fiber into small steps, the linear and nonlinear effects are assumed to act separately during each step. In general, smaller simulation step-size results in higher simulation accuracy at a cost of more simulation steps. The enhancement in the computational efficiency is mainly achieved by the fast Fourier transform (FFT), which is used for solving the higher order time derivatives for the fiber CD effect. Due to their simplicity for implementation and high computational efficiency, SSF based methods are used almost universally in commercial software packages, industry R&D, and academic research. To further enhance the computational efficiency, an analytical step-size selection formula was proposed to calculate variable step-size on the fly during simulation runs [12]. The key is to obtain approximately constant local error, or similar simulation error in each simulation step, so that there will be no computational waste from any simulation step. Combining the computational saving from the constant local error and the capability of step-size scaling to achieve the same global accuracy for varying optimizing parameter values, more than ten folds of computation saving can be obtained when compared to other step-size selection schemes such as the constant step-size rule or constant nonlinear rotation rule [12].

For the second order SSF method i.e., the symmetrized SSF method, approximately constant local simulation error can be achieved by using the following analytical formula [12] to select the simulation step-size,

Manuscript received September 17, 2014; revised January 27, 2015.
doi:10.12720/jcm.10.1.1-8

$$\gamma P_{max}(z)h(z)(D\Delta\lambda\Delta f h(z))^2=\Delta\xi. \quad (1)$$

In (1), γ represents fiber nonlinearity coefficient, D denotes the fiber dispersion parameter, $P_{max}(z)$ denotes the peak optical power of simulated waveform at propagation distance z, and the step-size h is written as $h(z)$ since h is calculated on the fly and thus it depends on z. The local error bound (LEB) $\Delta\xi$ should be understood as a bound on the pulse-width error resulted from simulation. For modern optical communication systems, the nonlinearity is moderate. So signal bandwidth $\Delta\lambda$ and Δf do not change significantly during simulation. Therefore, to estimate $h(z)$, the only parameter that needs to be calculated during the simulation is $P_{max}(z)$.

We have recently developed a simulation software package to implement the proposed simulation scheme [13]. The package can be divided into two segments. In the first segment, a trial value of the LEB is estimated by the preparation stage of the software run. Then multiple accurate LEB values can be obtained with only a few iterations of simulation runs using a signal pulse train for a limited number of transmitted symbols, to achieve a set of prescribed global error for a single span system. This segment of the software package is termed as LEB finding package in this paper. For long haul repeated span systems, if the desired global error is prescribed for an N span system, then during the process of deciding the correct $\Delta\xi$ value we only need to reduce the prescribed global error by N folds for the one-span based LEB finding software package. Once the desirable LEB is found, we can use the LEB for the second segment of the developed package [13], which is referred to as the main simulation package in this work. Note that the main simulation package is a multi-span simulation package. Both the LEB finding package and the main package are based on the scalar optical fiber channel model [2].

In this work we extend the previously developed LEB finding software package from single span to multi-spans. Furthermore, we extend the main package to include the vector optical fiber channel model that can model the dual polarized optical input and important polarization effects such as the random coupling of polarization states and polarization mode dispersion. More importantly, this is the first time that we extend our step-size optimization scheme to the vector channel simulation with dual polarization inputs, which is significant for the simulation of current and next generation coherent optical fiber communication systems. We start with an introduction of our implementation of the vector optical fiber channel model, with an emphasis on the proposed step-size selection rule. We then propose a hypothesis that by using the LEBs obtained from the scalar model based LEB finding package as the LEBs for the vector model based main simulation program, the same prescribed global simulation accuracy can be met. Detailed validation of our hypothesis will be presented using a dispersion managed polarization multiplexed QPSK (PM-QPSK) system. In addition, we compare the simulation efficiency of the proposed method to the constant step-size method, and we compare the evolution of step-size in vector simulation to that in scalar simulation to show that the step-size evolution has the similar trend. We conclude the paper with future work identified to further validate our results for different systems and settings.

II. Vector Optical Fiber Propagation Modeland Problem Formulation

We start with the nonlinear Schrödinger equation (NLSE) that governs the scalar optical fiber propagation model [2], [12],

$$\frac{dA(z,t)}{dz}=\left(\hat{D}+\hat{N}\left(A(z,t)\right)\right)A(z,t) \quad (2)$$

In (2), $\hat{D}=i(\beta_2\partial^2/\partial t^2-\alpha)/2$ denotes linear operator, $\hat{N}\left(A(z,t)\right)=-i\gamma|A(z,t)|^2$ denotes the nonlinear operator, where i is the imaginary number and $A(z,t)$ is the complex envelope of optical pulse. For simplicity, we can write $\hat{N}(A(z,t))$ as$\hat{N}$. Parameters β_2, α, γ, and t represent fiber group velocity dispersion, attenuation, nonlinearity, and retarded time, respectively. Note that $\gamma = 8a_0/9$ represents the fiber nonlinear coefficient when the polarization effects of the optical field are averaged during fiber propagation, and a_0 represents nonlinear coefficient that is measured from the propagation of an optical field aligned to fast or slow axis of a polarization maintaining fiber with the same waveguide and doping profile [2].

The coupled nonlinear Schrödinger (CNLS) equations as shown in (3) must be employed in order to model the propagation of dual vector optical input fields and polarization effects including the PMD effects [14, 15],

$$\frac{\partial\vec{A}}{\partial z}+ib\Sigma+b'\Sigma\frac{\partial\vec{A}}{\partial t}-\frac{i}{2}\beta_2\frac{\partial^2\vec{A}}{\partial t^2}+ia_0\times\left[\left|\vec{A}\right|^2\vec{A}-\frac{1}{3}\left(\overrightarrow{A^*}\sigma_2\vec{A}\right)\sigma_2\vec{A}\right]=0 \quad (3)$$

In (3), we have birefringence $b=(\beta_{0p}-\beta_{0o})/2$ and group delay per unit length $b'=(\beta_{1p}-\beta_{1o})/2$ with subscription p representing the preferred direction, and o for the orthogonally polarized wave. CD is modeled by $\beta_{2p}=\beta_{2o}=\beta_2$. In addition, $\vec{A}=(A_p,A_o)^t$ is a column vector with the two components representing the complex envelopes of the two orthogonally polarized optical fields. Note that the attenuation is absorbed in $\vec{A}$, t represent a retarded time with respect to the average time delay of the two polarized fields, and a signal processing or engineering convention is used for the definition of complex envelope and the definition of Fourier transform and the inverse Fourier transform. The matrix $\Sigma=\sigma_3\cos(2\theta)+\sigma_1\sin(2\theta)$ is defined in terms of the Pauli's matrices σ_1 to σ_3 as shown in [15], where θ is the rotation angle between the fixed coordinate system to a system that rotates with the principal axes of the fiber.

To simulate (3) we use a coarse step method for which the correctness was tested extensively by experiments and

theory [14]. With this method we assume that the optical fiber appears as polarization maintaining fiber within each coarse step that may be much larger than the fiber correlation length [15]. The two principle axes are denoted as *x* and *y* axes, and the two optical signal fields can be denoted as $A_x(z,t)$ and $A_y(z,t)$. After simulating signal propagation over a coarse step, the simulated optical fields will be scattered over the Poincaré sphere to take the large birefringence into the model, before entering the next coarse step. The step-size with the coarse step method is designated in an *ad hoc* way. For example, it may be a chosen constant or a constant plus a small random perturbation that is uniformly distributed.

The symmetrized split-step Fourier method will be used for simulation in each coarse step, simulating the linear operation on the first half step, followed by the nonlinear operation for the whole step, and finally the linear operation again on the second half step. Note that the nonlinear operation involves the nonlinear coupling among $A_x(z,t)$ and $A_x(z,t)$, $A_y(z,t)$ and $A_y(z,t)$, and $A_x(z,t)$ and $A_y(z,t)$ [14, 15]. For the main simulation, instead of using constant step-sizes, we propose to apply the similar step-size selection rule as in (1) for choosing the coarse step-sizes for the vector model, but with a modification of the peak power at a propagation distance $z_0$according to the following formula,

$$P_{max}(z_0,t) = \max_t \left(|A_x(z_0,t)|^2 + \left|A_y(z_0,t)\right|^2 \right) \qquad (4)$$

Note that this is the first time that an optimized and analytical step-size selection rule is applied to the coarse step method with the dual polarization inputs.

Now we propose the formulation of our research problems. The local error is related to system nonlinearity and dispersion, and is bounded by $\Delta\xi$ as shown by (1). As explained before, the only parameter that change significantly during signal propagation through e.g., a 100 km fiber segment, is the peak power $P_{max}(z)$. As a result, we have $h(z) = \Delta\rho/\sqrt[3]{P_{max}(z)}$, where $\Delta\rho = \Delta\xi/\sqrt[3]{\gamma(D\Delta\lambda\Delta f)^2}$ is approximately a constant since as explained before, $\Delta\lambda$ and Δf do not change significantly during simulation. The peak power decreases exponentially due to fiber attenuation, and thus the step-size increases during simulation of one fiber segment. When step-size follows the trend of $1/\sqrt[3]{P_{max}(z)}$, similar local error can be achieved for all the simulation steps in a single simulation run for scalar simulations [12]. This leads to higher computational efficiency compared to other prevalent step-size methods [12]. In this paper, we investigate the step-size trend for vector simulations to see if it will be similar to that for the scalar simulation. When the trend of $h(z) \propto 1/\sqrt[3]{P_{max}(z)}$ is confirmed, we can infer that in vector simulation similar local error can be achieved. Furthermore, we backup our claim by validating the computational efficiency enhancement via a comparison of the proposed step-size optimization method vs. the often used constant step-size method in vector simulations. The second problem is global error control for vector simulations. Currently there is no simulation accuracy control for vector simulations, so usually very small step-size is used to satisfy the waveform level simulation accuracy. The computational burden is very high for collecting statistics of interaction between nonlinearity and polarization effects [11]. Here for the vector simulation we propose a method of global error control by prescribing a target global error for a certain simulation need. To achieve the prescribed target global error, we need to find a LEB $\Delta\xi$ in order to use (1) and (4) for step-size calculation. For this purpose we propose to use the scalar magnitude of the vector signal, i.e., the square root of the optical power, as the input to the scalar model based LEB finding package. The scalar LEB finding package is able to find a $\Delta\xi$ that results in a prescribed global error. The hypothesis is that by using the thus-obtained $\Delta\xi$, we can achieve the same target global error for vector simulations, and so global accuracy control can be achieved. The third problem is to validate for vector simulations that global error for multi-span systems is a linear addition of the global error of individual spans. If verified we can infer that the computational improvement of the single span vector simulation, by using our step-size optimization rule, can be kept for multi-span simulations. In Section III we conduct single channel simulations for dispersion compensated links to systematically test the above described research items.

III. Results and Discussions

A. Simulation System Setup

We illustrate a 120 Gb/s PM-QPSK testing system in Fig. 1. The transmitter DSP block generates Nyquist BPSK signals for the four channels from XI to YQ. The detailed DSP blocks are similar to those in Fig.1 of [16]. The roll-off factor for raised cosine pulse shape is 0.1. The DSP sampling rate is two times of the symbol rate. The DAC resolution is 8-bits, and the DAC filter has a 3 dB bandwidth of 16 GHz. Arcsin stage is turned on to compensate the optical modulation switching curve [16]. A pre-emphasis filter compensates the DAC response by pre-emphasizing the high frequency components of the driving signal. The optical PM-QPSK signal is generated by using the nested parent/child modulators, where the child modulators generate optical BPSK signals while the parent modulators perform the I-Q mixing. The extinction ratio values of both child and parent modulators are 30 dB. The modulator 3 dB bandwidth is 26 GHz.

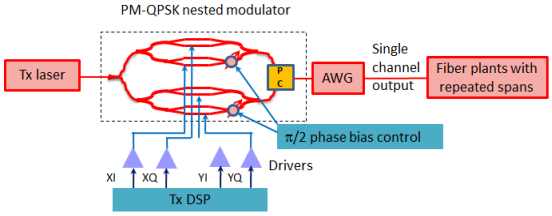

Fig. 1. Optical transmission system used in simulation. In the block diagram, Tx stands for transmitter, and PC is a polarization combiner.

The arrayed waveguide grating (AWG) follows the transmitter, and its transfer function is modeled as a super Gaussian 4th order filter with a 3 dB bandwidth of 40 GHz. The fiber plant includes repeated spans each with 100 km standard single mode fiber (SSMF) plus 17.7km dispersion compensating fiber (DCF) links. The carrier wavelength is 1545 nm. The launch power into SSMF is 6 dBm. Two stage Erbium doped fiber amplifiers (EDFAs) are used in each span, one at the end of the SSMF, and the other at the end of the DCF. The mid-span loss, i.e. the loss before the DCF segment, is controlled by variable optical attenuators such that the launch power into DCF is always 7 dB lower than that into the transmission fiber. The information bit sequence is a 4096-bit pseudorandom bit sequence. So there are 1024 symbols used in the simulation in this study. Simulation sampling rate is 480 GHz.

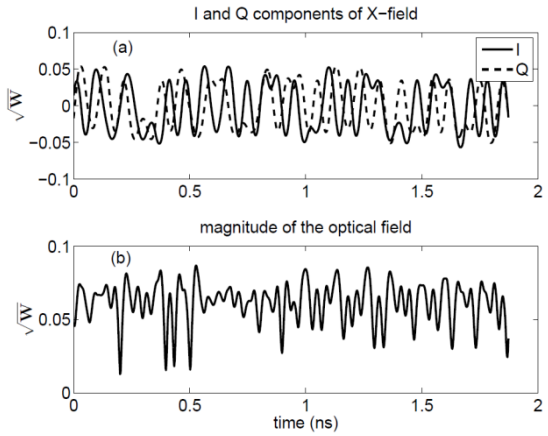

Fig. 2. Illustration of (a) the I/Q optical fields and (b) the magnitude of the optical field generated by the transmitter.

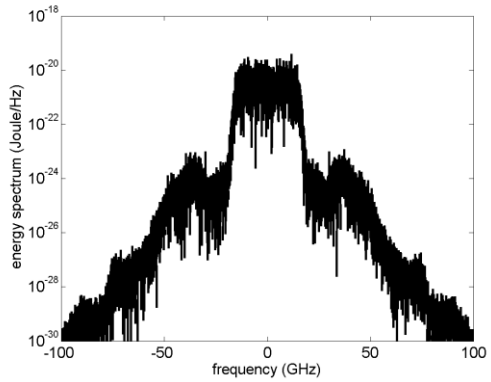

Fig. 3. Energy spectrum of the total optical field before the AWG.

In Fig. 2 we illustrate a part of the simulated time domain optical signal waveform before the AWG. The energy spectrum of the total optical field is illustrated by Fig. 3. From these figures we can see that the signal peak to average ratio is not very high before signal launch into the optical fiber, and the spectrum is well confined due to the small roll-off factor used in waveform generation via the transmitter DSP. During propagation, fiber CD and PMD cause large interfering pattern effects. We found that the peak to average power ratio (PAR) of the studied PM-QPSK is usually higher than the PAR of the scalar field. This justifies the use of $P_{max}(z_0, t)$ in (4) to achievethe prescribed global simulation accuracy when using the LEB values obtained from scalar simulation.

B. LEB Finding for Single Span and Multi-Span Systems

Now we use our scalar LEB finding package to identify LEBs for prescribed global error levels. We start with the single span system. The input signal to the scalar LEB finding package is the magnitude of the total optical field as illustrated in Fig. 2b. The details of LEB finding have been reported in [13] for single span systems. For the studied system, we find that when the step-size of the first step is 100 meters, the calculated LEB is about 1.6e-7. We choose this value as the trial LEB, and find that after respectively 4, 2, and 3 iterations, the prescribed global error targets of normalized standard deviation (*nsd*) = 1e-3, 1e-4 and 1e-5 are obtained with less than 10% variation [13]. The total numbers of simulation steps are respectively 16, 49, and 163. Recall that thensd isused as the criterion for simulation error [12],

$$nsd = \|A_0(L,t) - A_t(L,t)\| / \|A_{in}(0,t)\| \qquad (5)$$

In (5), $A_0(L,t)$ is the simulated scalar optical field using a certain $\Delta\xi$ and $A_t(L,t)$ is the "true" optical field which could be obtained by using a very small $\Delta\xi$ satisfying the desired accuracy for thetrue filed. Note that L is the total propagation distance, $A_{in}(0,t)$ is the input scalar optical field, and $\|A\|$ denotes the operation of$(\int |A|^2\, dt)^{1/2}$. Theobtained results are summarized in Table I.

TABLE I. LEB FINDING RESULTS FOR THE SINGLE SPAN SYSTEM

Key parameters	**Value(s)**
LEB for true solution	1e-10
LEB for trial solution	1.6e-7
Prescribed global error (GE) levels	[1e-3 1e-4 1e-5]
Number of iterations for GE convergence	[4, 2, 3]
Obtained GEs	[1.02e-31.06e-4 1.01e-5]
LEBs found to achieve GEs	[4.251e-3 1.34e-4 3.40e-6]
Number of steps in SSMF	[16 49 163]
Number of steps in DCF	[13 39 132]
Total Number of steps	[29 88 295]

As we explained in Section I, the LEB finding package has been extended to include multi-span cases. Three prescribed *nsd* levels are studied: 1e-3, 1e-4 and 1e-5. We simulate a 3-repeated-span system and a 12-repeated-span system with each span identical to the single span system we just discussed. The obtained results along with the single span results are plotted in Fig. 4. The blue curves with 'o' and 'x' markers represent the LEBs and the red curves with '+' and diamond markers represent obtained global simulation error in terms of *nsd*. Specifically, Figure 4a summarizes the single span results from Table 1. For the 3-span system, the required LEBs are 8.078e-4, 2.392e-5, and 1e-6 to achieve global error of respectively 1.06e-3, 1.03e-4, and 1.02e-5. This result

is shown in Fig. 4b. The ratios of the LEBs for single span system to those for 3-span system are respectively 5.26, 5.62 and 3.4, which are reasonable considering the theoretical ratio should be $(3/1)^{3/2}$= 5.2 with "(3/1)" representing the ratio of the number of spans, 3 in "3/2" representing the fact that the LEB is proportional toh^3, and 2 in "3/2" representing the fact that global simulation error is proportional toh^2[12]. To understand the scaling of the number of spans better, we scale the LEBs from the single span results and apply these scaled LEBs directly to the 12-span scalar simulations. The scaled LEBs are [1.023e-4 3.233e-6 8.179e-8], and the corresponding global error levels are [0.975e-3, 0.6e-4 0.352e-6]. The scaled LEBs and resulting global error are plotted using respectively curves with respectively 'x' and '+' markers in Fig. 4c. For comparison purpose, we plot the LEBs and the corresponding global error using the LEB finding program for the 12-span system with respectively circle and diamond markers in Fig. 4c. We can see the LEB finding program yields slightly larger LEBs since higher PAR may occur during 12-span simulation, such that even with slightly larger LEBs, the step-size may still be small enough to yield the prescribed global error. The study shows that by using the scaled LEBs from a single span LEB finding program, we are conservative in terms of obtaining slightly smaller global error than the prescribed one. The cost is slightly increased computation complexity: the extra computation needed in terms of the percentage of increase in the number of steps is ranging from 5.1% to 28.6% for the studied three global error levels.

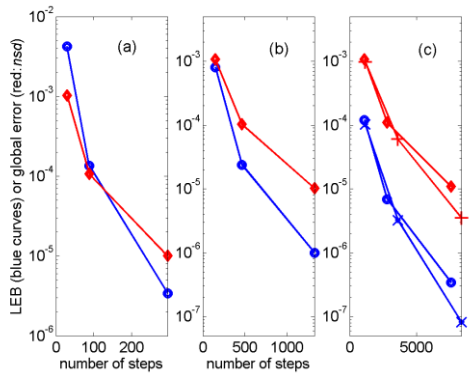

Fig. 4. LEB finding performance vs. number of total simulated steps for (a) single span system, (b) 3-span system, and (c) 12-span system.

C. The Performance of Satisfying Prescribed Global Accuracy: Single Span System

We use the obtained three LEBs from the single span LEB finding program as the LEBs for the main vector propagation simulation program. The global error *nsd* is modified for PM-QPSK system with coherent detection,

$$nsd = \sqrt{\frac{\int(|A_x(L,t) - A_{xt}(L,t)|^2 + |A_y(L,t) - A_{yt}(L,t)|^2)dt}{\int(|A_{xin}(0,t)|^2 + |A_{yin}(0,t)|^2)dt}} \quad (6)$$

In (6), $A_x(L,t)$ and $A_y(L,t)$ represent the simulated approximate solutions, $A_{xt}(L,t)$ and $A_{yt}(L,t)$ represent "true" solutions obtained using a small LEB for each saved step, and $A_{xin}(0,t)$ and $A_{yin}(0,t)$ are the inputs. We found that for the studied range of global error, the *nsd* from (6) is slightly larger than the *nsd* calculated using (5) where the scalar magnitude of optical field can be calculated from A_x and A_y.

Here we assume the optical fields $A_x(0,t)$ and $A_y(0,t)$ are aligned respectively with the fast and slow axis of the SSMF at the input to the studied span. We assume random polarization coupling in fibers with PMD = 0.1ps/$\sqrt{km}$ for both SSMF and DCF. Because each simulation step involves random polarization coupling, all the polarization scattering angles and step-sizes need to be saved for every coarse step. To simulate the true solution, we reload the saved polarization scattering angles and step-sizes, equally divide each step into 10 finer steps, and perform symmetrized SSF simulation over every finer step.

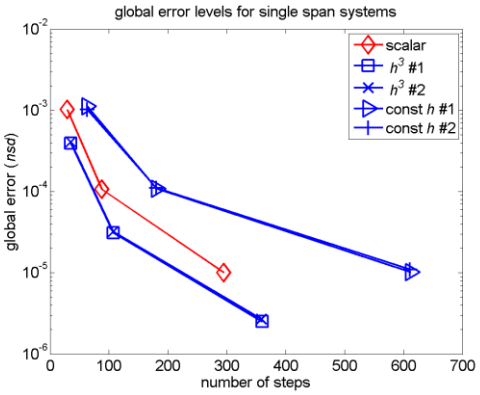

Fig. 5. Global error levels vs. number of steps for single span simulations.

The results from two simulations using two different sets of initial random seeds for the polarization scattering angles are summarized in Fig. 5. For comparison purpose, the single span scalar case is also plotted. One notable result is that for the two vector cases labeled as h^3 #1 and #2, the number of steps and the global error levels are almost identical. This result infers that for cross polarization systems such as PM-QPSK system, the peak power of the long simulated waveform only weakly depends on polarization coupling for a single dispersion compensated span. Another important result, as illustrated by the global error curves in Fig. 5, shows that by using the scaled LEBs from the scalar LEB finding program, we obtain slightly smaller global error than the intended global error. The cost is slightly increased computation complexity: the extra computation needed in terms of percentage of the increase in the number of steps is respectively 21%, 22%, and 22%, for the three prescribed global error levels. Since these values are uniform for the studied range of global accuracy, LEBs may be scaled to larger values to achieve the prescribed

global error levels. The results may infer that the PMD actually reduces the nonlinear effects in the studied system.

We also plotted the vector simulation results by using constant step-sizes for two different PMD realizations. These curves are labeled using const h #1 and #2. Comparing the gaps between the performance curves obtained using the proposed step-size optimization method and the constant step-size method, we find that for the studied global accuracy range the number of total required simulation steps is two times less for the proposed method than the constant step-size method, to achieve the same global error. As a result 100% of computational saving is achieved by using the proposed method for a single simulation run compared to the often used constant step-size method in vector simulations.

D. *The Performance of Satisfying Prescribed Global Accuracy: Multi-Span System*

We simulate the 12-span PM-QPSK system with two different sets of initial random seeds for polarization scattering. The PMD for both SSMF and DCF is $0.1\text{ps}/\sqrt{km}$. Prescribed global error is *nsd* = 1e-4, and the LEB and converged global error obtained from the 12 span scalar LEB finding program are respectively 6.93e-6 and 1.098e-6. Using the obtained LEB, the vector simulation results after the span number 1, 3, 5, 7, 9, and 12 are recorded. We find the random polarization scattering does not affect the simulation performance. For example, with one set of random seeds, the global error after 12 spans is 0.5355e-4 and the total number of simulation steps is 3400. While another set of random seeds yield a global error of 0.5352e-4 and the total number of steps of 3408. In contrast, the number of steps during the scalar LEB finding is 2801. The global error and the total number of simulation steps after span 1, 3, 5, 7, 9, and 12, for one set of random seeds, are summarized in Fig. 6. Unlike the scalar case, the linear growth of the global error vs. span number and total number of simulation steps is strict in the vector simulations, and the multi-span global error is approximately the sum of global error of individual spans. This shows that the computational efficiency for one span simulation can be maintained for multi-span simulation.

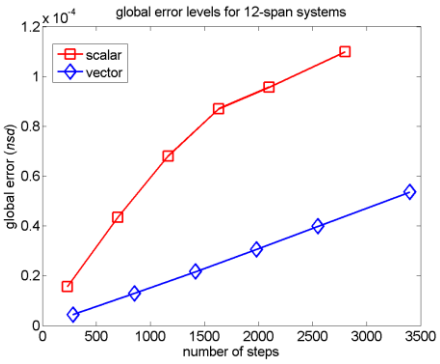

Fig. 6. Global error levels after span number 1, 3, 5, 7, 9, and 12 vs. the corresponding total number of accumulated steps.

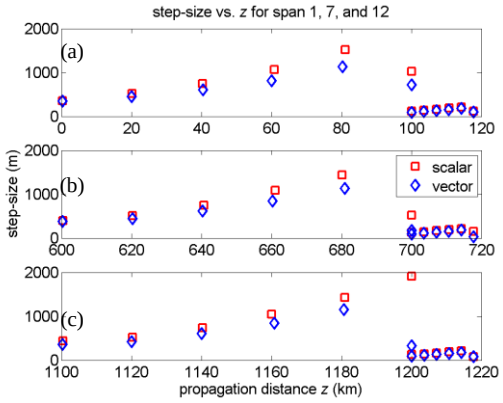

Fig. 7. Step-size vs. propagation distance for span number 1, 7, and 12 in respectively (a), (b), and (c).

We also plot the varying step-size values vs. propagation distance for span number 1, 7, and 12 respectively in Fig. 7a, b and c. Six steps each are chosen for the SSMF and the DCF in the studied span. The six steps include the first step, the last step, and the in-between steps at approximately uniform distance intervals in each fiber. For spans 7 and 12, the propagation distance on the y-axis starts from distance by only counting the accumulated SSMF length. After the SSMF, the DCF length is simply appended in the plots. The step-size of the last step may show seemingly unusual decrease. This is because the last step needs simply make up the fixed fiber length in the simulation. Fig. 7 shows that the step-size in vector simulation is slightly smaller than in scalar simulation, resulting in a slightly larger number of steps needed in simulation. The extra computation needed in terms of percentage of the increase in the number of steps is 21.7%, 21.6%, and 21.4% after span number 1, 7, and 12, respectively. This is similar to the results from the single span simulation: since these values are uniform for the studied range of global accuracy, LEBs may be scaled to larger values to achieve the prescribed global error levels. Another key result as evidenced by Fig. 7 is that evolution of step-size in vector simulation follows the same trend of that in scalar simulation, from which we infer that approximately constant one-step or local error is achieved in the vector simulation.

IV. Conclusions and Future Work

We have shown by using the LEBs obtained from the scalar model based LEB finding program, the prescribed global accuracy can be satisfied for the studied PM-QPSK system in the simulation of vector optical field propagation through multi-span dispersion managed SSMF + DCF links. The key techniques to the conducted vector simulation are 1) the coarse step algorithm and 2) the proposed analytical step-size selection rule. The coarse step algorithm allows the use of much larger step-size than the fiber PMD correlation length in the simulation, while our step-size selection rule leads to a slightly conservative simulation performance that meets

the prescribed global error at a cost of about 20% more numbers of simulation steps than the scalar simulation counterpart (but recall that the scalar simulation using our optimized step-size selection rule has significant computational savings compared to other step-size selection schemes). Comparing to the constant step-size method which is often used in vector simulations, the proposed method achieves 100% enhancement of the computational efficiency in terms of required simulation steps for the same global error. Finally, we found that the optimized step-size calculated on the fly during simulation is not significantly affected by the random polarization coupling of the cross polarized fields. However, due to the randomness of the data symbols in the two cross polarized channel and the large CD present in the link, the interfering pattern is richer than the scalar counterpart. This may increase the PAR and result in the slightly decreased step-size and reduced global error. In the future work we plan to conduct similar study with smaller PMD length scale using increased PMD values. Both the CD and PMD effect may affect simulation accuracy differently. We will investigate uncompensated links without inline DCFs. In addition, we will validate our results against wavelength division multiplexing (WDM) PM-QPSK systems which have a much wider bandwidth than single wavelength channel systems studied here.

ACKNOWLEDGMENT

S. Karri also thanks the support for his Research Assistant support during summer 2013 from Dean of College of Science, Engineering and Technology at Minnesota State University.

REFERENCES

[1] M. C. Jeruchim, P. Balaban, and K. S. Shanmuga, *Simulation of Communication Systems: Modeling, Methodology and Techniques*, 2nd edition, New York: Springer, 2000.

[2] G. P. Agrawal, *Nonlinear Fiber Optics*, 5th edition, New York: Elsevier Academic Press, 2012.

[3] M. I. Hayee and A. E. Willner, "Pre- and post-compensation of dispersion and nonlinearities in 10-Gb/s WDM systems," IEEE Photon. Tech. Lett., vol. 9, no. 9, pp. 1271–1273, September 1997.

[4] E. A. Golovchenko, A. N. Pilipetskii, N. S.Bergano, C. R.Davidson, *et al*., "Modeling of transoceanic fiber-optic WDM communication," *IEEE J. of Sel. Top. Quantum Electron.*, vol. 6, no. 3/4, pp. 337-347, March/April 2000.

[5] P. A. Humblet and M. Azizoglu, "On the bit error rate of lightwave systems with optical amplifiers," *J. Lightw. Technol.*, vol. 9, no. 11, pp. 1576–1582, November 1991.

[6] N. S. Bergano, F. W. Kerfoot, and C. R.Davidson, "Margin measurement in optical amplifier systems," *IEEE Photon. Technol. Lett.*, vol. 5, no. 3, pp. 304-306, March 1993.

[7] Q. Zhang, C. R. Menyuk, R. Bajracharya, M. I. Hayee, H. W. Huang, and A. Miner, "On the gaussian approximation and margin measurements for optical DPSK systems with balanced detection," *IEEE J. Lightw. Technol.*, vol. 28, no. 12, pp. 1752-1760, June 2010.

[8] E. Ip, A. P. T. Lau, D. J. F. Barros, and J. M. Kahn, "Coherent detection in optical fiber systems," *Opt. Express*, vol. 16, no. 2, pp. 753-791, January 2008.

[9] Q. Zhang, G. Namburu, S. Karri, and P. V. Mamyshev, "Optimization of transceiver signal clipping in polarization multiplexing QPSK (PM-QPSK) systems with Nyquist signals," in *Proc. IEEE Photonics Conference*, Bellevue, 2013, pp. 517-518.

[10] V. Curri, P. Poggiolini, G. Bosco, A. Carena, and F. Forghieri, "Performance evaluation of long-haul 111 Gb/s PM-QPSK transmission over different fiber types," *IEEE Photon. Tech. Lett.*, vol. 22, no. 10, pp. 1446-1448, October 2010.

[11] P. Serena, N. Rossi, O. Bertran-Pardo, J. Renaudier, A. Vannucci, and A. Bononi, "Intra-versus inter-channel PMD in linearly compensated coherent PDM-PSK nonlinear transmissions," *J. Lightw. Technol*, vol. 29, no. 11, pp. 1691–1700, April 2011.

[12] Q. Zhang and M. I. Hayee, "Symmetrized SSF scheme to control global simulation accuracy in fiber optic communication systems," *J. Lightw. Technol*, vol. 26, no. 2, pp. 302-316, January 2008.

[13] Q. Zhang, S. Shrestha, R. Rashid, S. Karri, and M. Khaliq, "An efficient split-step optical fiber simulation package with global simulation accuracy control," in *Proc. IEEE/CIC International Conference on Communications in China*, Xi'an, 2013, pp. 158-164.

[14] S. G. Evangelides, L. F. Mollenauer, J. P. Gordon, and N. S. Bergano, "Polarization multiplexing with solitons," *IEEE J. Lightw. Technol.*, vol. 10, no. 1, pp. 28–35, January 1992.

[15] D. Marcuse, C. R. Menyuk, and P. K. A. Wai, "Application of the Manakov-PMD equation to studies of signal propagation in optical fibers with randomly varying birefringence," *IEEE J. Lightw. Technol.*, vol. 15, no. 9, pp. 1735–1746, September 1997.

[16] V. Curri, A. Carena, G. Bosco, P. Poggiolini, and F. Forghieri, "Optimization of DSP-based Nyquist-WDM PM-16QAM transmitter," in *Proc. ECOC*, Amsterdam, 2012.

Qun Zhang, received the B.S. degree from the Department of Optics in Shandong University in 1993, and the M.S. degree in Solid State Physics in the Institute of Crystal Materials, Shandong University in 1996. He received the Ph.D. degree in Electrical Engineering from the University of Virginia in 2001. Since August 2000he has worked in core R&D groups in companies including PhotonEx, Corvis (currently part of Level 3 Communications), and Tyco Telecommunications, mainly on modelling (with experimental validation), simulation, and design of 40 Gb/s optical communication subsystems and systems. Dr. Zhang joined Minnesota State University, Mankato in 1996 and he is currently a Professor with the Department of Electrical and Computer Engineering, Minnesota State University, Mankato, MN, USA. Dr. Zhang was a consulting engineer for Oclaro Inc. during the last four years, and he is a technology consultant for Micropoint Bioscience Inc.His research focuses on modeling and simulation of photonics devices and communication systems, and digital signal processing for coherent optical fiber communications and medical devices.

Santosh Karri, is a graduate student at Minnesota State University, Mankato. His research interests include optical coherent transceivers and simulation of signal propagation through the single mode optical fiber.

Muhammad Khaliq, obtained his Ph. D. from University of Arkansas, Fayettevile. He is currently a Professor in Department of Electrical and Computer Engineering and Technology, Minnesota State University, Mankato Minnesota. Dr. Khaliq started the Microelectronics program, teaches courses on Microelectronics and Nanoelectronics, and directs the Microelectronics Fabrication Lab. He is a senior member of IEEE.

Liudong Xing, received the B.E. degree in computer science from Zhengzhou University, China in 1996, and the M.S. and Ph.D. degrees in electrical engineering from the University of Virginia in 2000 and 2002, respectively. She is currently a Professor with the Department of Electrical and Computer Engineering, University of Massachusetts

(UMass) Dartmouth, USA. She is an Associate Editor for International Journal of Systems Science and Assistant Editor-in-Chief for International Journal of Performability Engineering. Dr. Xing is the recipient of the 2010 Scholar of the Year Award, and 2011 Outstanding Women Award of UMass Dartmouth and the IEEE Region 1 Technological Innovation (Academic) Award in 2007. She is also the co-recipient of the Best Paper Award at the IEEE International Conference on Networking, Architecture, and Storage in 2009. Her research focuses on reliability analysis of complex systems and networks. Dr. Xing is a senior member of IEEE.

M. Imran Hayee, received his Ph. D. from University of Southern California, Los Angeles in Dec 1998. After completing his Ph.D., he worked in Forward Looking Work Group of Tyco Submarine Systems (formerly known as Bell Laboratories) in New Jersey for two years and then joined a start-up company (currently part of Level 3 Communications) working on research and development of the state-of-the-art telecommunications products. Four years later, he joined University of Minnesota Duluth (UMD) in Fall 2004. Since then, he has continued his research work on optical fiber communications systems, digital signal processing, intelligent transportation systems, and medical instrumentation. Dr. Imran Hayee is currently a professor in the electrical engineering department at the University of Minnesota Duluth. Dr. Hayee holds 15 US patents and has published 55 research articles in distinguished journals and conferences. He is senior member of IEEE and was the recipient of UMD Chancellor's distinguished award for excellence in research for the year 2011-2012.